JOURNAL OF SPACECRAFT AND ROCKETS
Vol. 48, No. 1, January–February 2011

Ionic Liquid Dual-Mode Spacecraft Propulsion Assessment

Brian R. Donius* and Joshua L. Rovey†
Missouri University of Science and Technology, Rolla, Missouri 65409

DOI: 10.2514/1.49959

Analytical and numerical investigations of the performance of a series of potential dual-mode propulsion systems using ionic liquids are presented. A comparison of the predicted specific impulse of ionic liquids with hydrazine and unsymmetrical dimethylhydrazine shows that ionic liquid fuels have a 3–12% lower specific impulse when paired with a nitrogen tetroxide oxidizer. However, when paired with hydroxylammonium nitrate oxidizer, the specific impulse of the ionic liquids is 1–4% lower than that of hydrazine and unsymmetrical dimethylhydrazine paired with nitrogen tetroxide. Analytical investigation of an electrospray electric propulsion system shows that ion extraction in the pure ion regime provides a very high specific impulse, outside the optimum range for potential missions. Results suggest a deceleration grid, a lower ion fraction, or emission of higher solvated states is required. Analysis of a dual-mode ionic-liquid-propelled spacecraft shows that the electric propulsion component determines the overall feasibility compared with current technology. Results indicate that the specific power for an ionic liquid electrospray system must be at least 15 W/kg in order for a dual-mode ionic liquid system to compete with traditional hydrazine and Hall thruster technology.

Nomenclature

e	=	fundamental charge, Coulomb
F_{tu}	=	Allowable material strength, GPa
g_0	=	gravitational constant, m/s^2
H_{fg}	=	gaseous heat of formation
I_{emit}	=	current for a single emitter, A
K	=	ratio of specific heats
m	=	accelerated particle mass, kg
MW	=	molecular weight, g/mol
M_{ct}	=	mass of chemical propellant tank, kg
M_{et}	=	mass of xenon electric propellant tank, kg
M_p	=	mass of propellant, kg
$\dot{m}_{\text{emit}}$	=	mass flow rate of single emitter, kg/s
m_{f1}	=	mass of spacecraft after chemical burn, kg
m_{f2}	=	mass of spacecraft after electrical thrusting, kg
$\dot{m}_{\text{tot}}$	=	total mass flow rate, kg/s
m_0	=	full spacecraft mass, kg
N_{emit}	=	number of emitters
P_c	=	combustion chamber pressure, kPa
P_{in}	=	input power, W
P_t	=	propellant tank pressure, kPa
P_2/P_1	=	ratio of nozzle exit pressure to combustion chamber pressure
R	=	universal gas constant, kJ/kmol K
R_A	=	ion fraction
T	=	thrust, N
t	=	time required to change velocity, s
T_{chem}	=	thrust of chemical propulsion, N
T_{elec}	=	thrust of electric propulsion, N
T_m	=	melting temperature, K
T_o	=	chamber temperature, K
V_e	=	exit velocity, m/s
V_{xe}	=	volume of xenon propellant, m^3
ΔV	=	change in velocity, m/s
$\Delta\varphi$	=	change in electric potential, Volt
ε	=	nozzle expansion ratio
η_{sys}	=	system efficiency
ρ_m	=	density of tank structural material, kg/m^3
ρ_p	=	density of chemical propellant, kg/m^3

Received 19 March 2010; revision received 1 September 2010; accepted for publication 10 September 2010.

*Graduate Research Assistant, Aerospace Plasma Laboratory, Mechanical and Aerospace Engineering, 160 Toomey Hall, 400 West 13th Street. Student Member AIAA.

†Assistant Professor of Aerospace Engineering, Mechanical and Aerospace Engineering, 292D Toomey Hall, 400 West 13th Street. Senior Member AIAA.

I. Introduction

THE combination of high-thrust chemical and high-specific impulse electric propulsion (EP) into a single dual-mode system has the potential to greatly enhance spacecraft mission capability. Ideally, the combined system would share both hardware and propellant to provide the greatest reduction in system mass and maximum spacecraft flexibility. This paper describes and reviews the current state of the art in dual-mode propulsion and ionic liquids. It then quantifies the anticipated chemical and electric thruster performances of popular ionic liquids. Finally, it summarizes predicted propulsion performance and identifies three potential dual-mode systems. These dual-mode systems are compared with two traditional systems.

An ionic liquid is either an organic or inorganic salt in a molten (liquid) state. Because of its molten state, the cation and anion of the salt dissociate, but the overall liquid remains quasi neutral. All salts obtain this state if heated to the proper temperature, but there is a subgroup known as room-temperature ionic liquids that can remain liquid at or below 293 K. Although ionic liquids have been known since 1914, recent developments in chemistry have increased the number of known ionic liquids into the hundreds [1]. The exact mechanism for this molten salt behavior has yet to be identified, making the prediction of ionic liquid properties difficult. In general, however, ionic liquids have high conductivity, high viscosity, and negligible vapor pressure.

Current research is investigating ionic liquids as replacements for traditional explosives and rocket propellants [2,3] and volatile industrial solvents in chemical processing [2]. Although most professionals consider ionic liquids benign, a large group of researchers recently highlighted the combustibility of many ionic liquids as they approached decomposition temperature [4]. This work also pointed out that combustion of several ionic liquids becomes drastically more vigorous when the ionic liquids are sprayed rather than combusted as a pooled sample. Other articles have suggested that ionic liquid hydroxylammonium nitrate (HAN) may be used as a monopropellant substitute for hydrazine [5–7]. These analyses show that the performance of HAN in both pure and mixed forms is similar to that of hydrazine. In addition, hypergolic behavior has been reported for

several ionic liquids when combined with traditional space storable oxidizers [8–10].

Ionic liquids have also been investigated as electrospray propellants [11–13]. Ionic liquids for electrospray application were initially investigated because of their low vapor pressure. Previous electrospray liquids had relatively high vapor pressure and would boil off the emitter, resulting in a very inefficient impulse when no impulse was required. Interest in this application of ionic liquids has prompted multiple studies exploring plume emission of electrospray ionic liquids. Results have shown that an ionic liquid spray can approach a purely ionic regime (PIR) of emission similar to that found in field emission EP [13].

The main goal of a dual-mode propulsion system is to reduce spacecraft mass and enhance flexibility through the use of common system resources. Examples of common resources include hardware and propellant. The modes of propulsion can be characterized by the tasks to be performed by the propulsion system during a mission. These tasks include, but are not limited to, high-thrust orbit transfer maneuvers, low-thrust stationkeeping, low-thrust orbital transitions, and precision low-thrust pulses for attitude control. Although the dual-mode concept has been discussed in the academic community for quite some time, focused research has been nearly nonexistent.

One of the few instances in which dual-mode propulsion has been applied is the Mars Global Surveyor [14]. However, this system consisted of two chemical systems: bi- and monopropellant thrusters. The system was developed on a tight budget and a rushed schedule dictated by the loss of the Mars Observer craft. The system consisted of a common fuel bipropellant thruster and a catalytic monopropellant thruster. The bipropellant thruster was used in conjunction with aerobraking to bring the probe into orbit around Mars, and the monopropellant system was used for attitude control. The propellant common to both thrusters was hydrazine [14], which permitted the integration of three identical and readily available tanks, thus reducing costs. Dual-mode propulsion was selected for this mission, based not on improved performance but on a desire to speed up development, cut costs, and ease integration issues presented by the smaller size of the Delta II launch vehicle selected for the mission. Although the Mars Global Surveyor does represent a dual-mode system, its use of traditional hypergolic propellants and catalyst monopropellant thrusters leaves little room for improved performance; therefore, new concepts for dual-mode propulsion are investigated.

The following sections focus on analyzing the potential benefits of an ionic liquid-based dual-mode propulsion system. First, in Sec. II, the chemical propulsion performance of select ionic liquid fuels are investigated and compared with their conventional counterparts. Then the EP capabilities of an ionic liquid electrospray system operating in the PIR are parametrically investigated in Sec. III. In Sec. IV, a parametric investigation of an ionic liquid dual-mode propulsion system is described and compared with conventional thruster technology. Section V presents the conclusions of the analysis.

II. Chemical Propulsion Analysis

The NASA John H. Glenn Research Center at Lewis Field's Gordon–McBride Chemical Equilibrium with Applications (CEA) code is used to analyze the chemical combustion and rocket performance of multiple bipropellant combinations [15]. Specifically, ionic liquid fuels and oxidizers are paired with conventional fuels and oxidizers to determine rocket performance.

A. Fuels Investigated

Ten different ionic liquids are selected for analysis based on data available in the literature. To evaluate the capabilities of an ionic liquid fuel in a chemical propulsion system, the fundamental properties, such as the heat of formation, the melting point, and the density, must be determined. Because investigation of the combustion properties of ionic liquids has only recently begun to receive attention, knowledge of the heat of formation of these liquids is limited. Therefore, 1-butyl-3-methylimidazolium dicyanamide (BIMDCA) and 1-butyl-3-methylpyrrolidinium dicyanamide are selected as two of the ionic liquid fuels because of the availability of heat of formation data. Additionally, BIMDCA has been reported to have hypergolic reactions with standard storable oxidizers [10]. The heat of formation of both dicyanamide ionic liquids was determined through calorimeter tests and calculations using the quantum chemistry program Gaussian 3 [16,17]. Reported results show a difference of approximately 1% between calculated and experimental data. Heats of formation for eight energetic ionic liquids based on 5-aminotetrazolate have also been determined [18]. To permit a comparison with current space storable propellants, hydrazine and unsymmetrical dimethylhydrazine (UDMH) are also evaluated. Table 1 summarizes all thermodynamic data for these fuels.

B. Investigated Oxidizers

Four oxidizers are selected for the combustion analysis. One of the oxidizers, HAN, is an ionic liquid. The other three are common in

Table 1 Thermochemical data for fuel and oxidizers investigated in this study

Fuel No.	Fuel Name	Formula	H_{fg}, kJ·mol^{-1}	Density, g·cm^{-3}	Melting point, K
	Hydrazine	N_2H_4	——	1.01	275
	UDMH	$C_2H_8N_2$	——	0.79	216
1	BIMDCA	$C_{10}H_{15}N_5$	363.40	1.06	267
2	1-Butyl-3-methylpyrrolidinium dicyanamide	$C_{11}H_{20}N_4$	218.90	1.02	223
3	Hydrazinium 5-aminotetrazolate	CH_7N_7	383.60	1.48	398
4	Guanidinium 5-aminotetrazolate	$C_2H_8N_8$	205.40	1.54	399
5	Aminoguanidinium 5-aminotetrazolate	$C_2H_9N_9$	302.30	1.51	366
6	Guanylguanidinium 5-aminotetrazolate	$C_3H_{10}N_{10}$	306.90	1.41	414
7	4-Amino-1H-1,2, 4-triazolium 5-aminotetrazolate	$C_3H_7N_9$	565.00	1.62	387
8	4-Amino-1-methyl-1, 2,4-triazolium 5-aminotetrazolate	$C_4H_9N_9$	546.00	1.46	249
9	4-Amino-1-ethyl-1, 2,4-triazolium 5-aminotetrazolate	$C_5H_{11}N_9$	523.40	1.39	235
10	1,5-Diamino-4-methyl-1,2,3,4-tetrazolium 5-aminotetrazolate	$C_3H_9N_{11}$	655.10	1.57	444
		Oxidizers			
	NTO	N_2O_4	——	1.44	261.95
	WFNA	HNO_3	——	1.33	231.6
	IRFNA	$83\%HNO_3 + 14\%N_2O_4 + 2.4\%H_2O + .6\%HF$	——	1.59	216
	HAN	NH_3OHNO_3	−79.68	1.83	316.05

current state-of-the-art chemical rocket systems; these are nitrogen tetroxide (NTO), white fuming nitric acid (WFNA), and inhibited red fuming nitric acid (IRFNA). NTO is a highly toxic, storable space oxidizer with extensive flight heritage and, in most reactions, it provides the best performance. WFNA is essentially pure nitric acid doped with a small percentage of hydrofluoric acid to permit storage in a variety of container materials. In general, WFNA does not perform as well as NTO; however, although it is corrosive, it is relatively benign. In terms of percentage by mass, IRFNA is 83% HNO_3, 14% N_2O_4, 2.4% H_2, and 0.6% HF. In general, IRFNA's performance is the same as that of WFNA, but its melting point is much lower. The ionic liquid HAN is selected because of the aforementioned interest in ionic liquid-based monopropellant systems. For combustion analysis, HAN is considered as an oxidizer in a pure liquid state at 316.05 K. The thermodynamic data for the oxidizers are summarized in Table 1.

C. Performance Criteria and Simulations

The measures of performance selected for investigation here are specific impulse (ISP), density impulse, and storability. ISP is defined as the thrust per unit weight flow rate of propellant; it indicates how efficiently a system uses propellant. For ideal flows, it is determined from [19]

$$\text{Isp} = \frac{\sqrt{[2K/(K-1)](RT_0/\text{MW})[1-(P_2/P_1)^{(K-1)/K}]}}{g_0} \quad (1)$$

The pressure ratio in Eq. (1) is determined by solving the transcendental equation, assuming a nozzle area ratio ε:

$$1/\varepsilon = \left(\frac{K+1}{2}\right)^{1/(K-1)} \left(\frac{P_2}{P_1}\right)^{1/K} \sqrt{\frac{K+1}{K-1}\left[1-\left(\frac{P_2}{P_1}\right)^{(K-1)/K}\right]} \quad (2)$$

Density impulse takes into account how easily the oxidizer–fuel combination can be stored. For this project, the storability of the propellant is described qualitatively as the need for additional heating or cooling of the propellant to maintain liquid phase in the storage tanks. Storability is important for reducing strain on the power system of the satellite and preventing excessive propellant loss due to boil off. For this study, storability is defined quantitatively as the ratio of the melting point temperature of hydrazine to the melting point temperature of the fluid:

$$\text{Storability} = \left(\frac{T_{m,\text{N}_2\text{H}_4}}{T_{m,\text{Fluid}}}\right) \quad (3)$$

A value greater than one indicates that a propellant is at least as storable as hydrazine, whereas a value less than one indicates that additional heating of the propellant is required. These measures of performance can be determined only if the chemical composition and thermodynamic state of the exhaust stream from the rocket combustion chamber are known.

The NASA CEA code is used to determine the performance of each propellant combination. This program has been under continual development since the late 1950s and enables the user to determine equilibrium composition and adiabatic flame temperature for any reaction [15]. A recent addition to the program also allows the user to define a new fuel given the heat of formation and molecular composition. Since the gaseous heat of formation is required, the energy needed to convert the propellants from a liquid to a gas phase is neglected. A series of 1536 simulations are performed using CEA by varying P_c, the equivalence ratio, and the propellant combination for a fixed expansion ratio ε of 40.

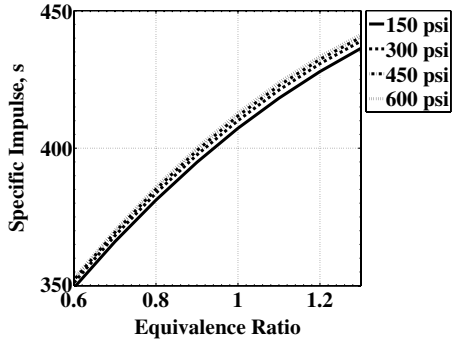

Fig. 1 Effect of chamber pressure on ISP for H_2/LOX.

D. Chemical Performance Estimation Results

The chamber pressure is varied between 150 and 600 psia, because these are typical levels in onorbit engines [20]. Figure 1 shows performance varies little with chamber pressure. This is to be expected as temperature, not pressure, is the primary driving force for dissociation; thus, the relatively small variations in the chamber pressure examined have little effect on the molecular weight of the gas and, thus, the ISP. Therefore, all subsequent analyses are restricted to the 300 psia case.

For the 48 propellant combinations, the mixture ratio is varied between 0.6 and 1.3 to determine the peak performance for each combination using CEA's combustion (enthalpy and pressure) case in concert with Eqs. (1) and (2), resulting in the frozen flow ISPs for each combination. An equivalence ratio of unity (stoichiometric) represents the point of complete combustion. Generally, peak performance is far to the right of the stoichiometric condition. This result is common for rocket performance, because as excess fuel is introduced to the system, molecular weight decreases faster than chamber temperature. Tables 2 and 3 summarize the results for all oxidizer–fuel combinations. The performance values are scaled with respect to the peak performance of hydrazine when combined with NTO (333 s and 406 g·s/cm^3). For example, the ISP of UDMH-NTO is 97% of that obtained for hydrazine-NTO.

Table 2 Summary of chemical propulsion: NTO and HAN oxidizers

	NTO		HAN		
Fuel	ISP	Density impulse	ISP	Density impulse	Storability
Hydrazine	1.00	1.00	1.03	1.14	1.00
UDMH	0.97	0.85	1.01	0.97	1.27
1	0.88	0.91	0.99	1.13	1.03
2	0.94	0.95	0.99	1.11	1.23
3	0.96	1.16	1.00	1.36	0.69
4	0.90	1.10	0.96	1.35	0.69
5	0.92	1.11	0.97	1.34	0.75
6	0.91	1.07	0.97	1.29	0.66
7	0.93	1.16	0.98	1.40	0.71
8	0.93	1.12	0.98	1.33	1.10
9	0.93	1.09	0.98	1.31	1.17
10	0.94	1.16	0.98	1.38	0.62

Table 3 Summary of chemical propulsion: IRFNA and WFNA oxidizers

	IRFNA		WFNA	
Fuel	ISP	Density Impulse	ISP	Density Impulse
Hydrazine	0.96	1.00	0.96	0.92
UDMH	0.93	0.85	0.93	0.79
1	0.90	0.96	0.90	0.88
2	0.90	0.95	0.90	0.87
3	0.93	1.18	0.93	1.07
4	0.88	1.13	0.88	1.00
5	0.89	1.14	0.89	1.02
6	0.88	1.09	0.88	0.98
7	0.90	1.20	0.90	1.08
8	0.90	1.14	0.90	1.03
9	0.90	1.11	0.90	1.01
10	0.91	1.19	0.91	1.07

Results show that hydrazine and UDMH provide higher ISPs than any of the ionic liquids investigated here, regardless of the oxidizer. However, in these simulations, hydrazine and UDHM combustion with HAN oxidizer provides higher ISPs than when combusted with NTO. With NTO oxidizer, the ionic liquid fuels have 3–12% lower ISPs than that of hydrazine and UDMH. Results show that NTO performs better than IRFNA and WFNA as an oxidizer for any given fuel, with the single exception of BIMDCA, which has only a small gain of 5 s ISPs. IRFNA and WFNA perform almost identically for all propellant combinations. When combined with HAN for ideal combustion, all fuels perform better; however, no ionic liquid HAN combination performs better than the baseline hydrazine–NTO case. The prediction that HAN performs better than NTO warrants further investigation.

In terms of density impulse, the ionic liquids perform better than traditional propellants, especially when combined with IRFNA and HAN. This improved performance is due to the greater density of the ionic liquids in comparison with that of hydrazine and UDMH. Density impulse indicates how easily an oxidizer–fuel combination can be stored. High density makes these propellant combinations ideal for small-volume budgeted systems with proportionally high mass budgets.

The analysis indicates that storability of ionic liquids is a major difficulty. Propellants 1, 2, 8, and 9 show storability equal to or greater than that of hydrazine. The remaining six propellants are not storable space propellants; therefore, they are dropped from consideration in the remainder of the study. With a storability factor of 0.87, HAN is not necessarily a storable propellant. However, because it is substantially closer to hydrazine than any other ionic liquid that failed the criteria (next closest is 0.75), HAN is the subject of further analysis.

E. Error Analysis

Although CEA is highly regarded for its predictive capabilities, its performance predictions must still be assessed for accuracy. To quantify the difference in the code performance predictions and real systems, a series of test cases are used to compare the predictions with actual engine performance for systems found in the Chemical Propulsion Information Agency (CPIA) engine manual. Given the mixture ratio, expansion ratio, and chamber pressure, the predicted ISP for equilibrium flow is compared with the actual performance (Fig. 2).

The error present in the analysis is difficult to quantify, but its sources are readily understood. First, the theory used in the design of CEA has some limitations, and numerical error exists no matter which methods are used. Thus, there is an inherent error present in CEA itself. Values of heat of formation for each of the ionic liquids examined have experimental or theoretical errors associated with them, depending on the methods used. The test stand data retrieved from the CPIA have experimental errors associated in the measurement of thrust and mass flow rate; thus, error is present in the ISP reported.

Quantification of the error present in CEA represents an extensive research project unto itself and is not conducted here. The error present in the CPIA engine test data is impossible to determine. The data represent the culmination of dozens of tests conducted by hundreds of individuals over the course of decades, with varying levels of documentation. Thus, no concrete numbers for experimental error can be defined for the CPIA data. However, the effect of error present in the heat of formation used to determine chemical performance can be quantified. For example, the value for heat of formation of fuel 2 has a reported experimental error of ± 3.4 kJ/k mol. By considering this variation in heat of formation, the resultant error in frozen flow ISPs for fuel 2 is ± 0.06 s. Since the error present in the inputs is negligible, and the errors associated with the test stand data and CEA are not readily possible or readily quantified, only a comparison of CEA to test stand data is possible. Thus, this does not represent an actual quantification of error but only a method for a more conservative estimate of performance.

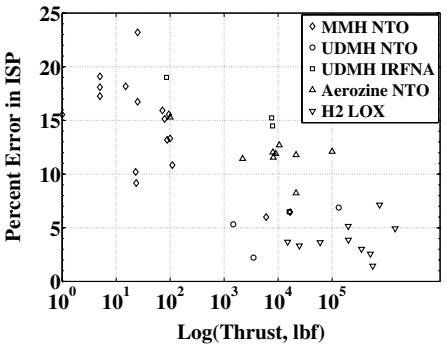

Fig. 2 Percent difference between CEA and test engine data (MMH denotes monomethylhydrazine).

Figure 2 shows that, as the thrust level increases, the accuracy of the simulation increases; this occurs because a larger thrust chamber dictates that a smaller percentage of the fluid is exposed to the nonisentropic effects of a high heat transfer rate and boundary layers that develop along the walls of the chamber and nozzle. For engines with thrust levels below 100 lbf (typical of small spacecraft), the ISP values predicted by CEA are 15.6% higher on average than those indicated by the test data, with a standard deviation of 3.7%. A 19.3% reduction in ISPs from the data shown in Tables 2 and 3 is used for the remainder of the study to allow for a more conservative estimate of the ISPs, and it represents a factor of safety of one standard deviation.

III. Electrical Performance

A dual-mode propulsion system with a common propellant must have an EP system that can operate with a combustible fuel. This investigation focuses on ionic liquids as possible EP propellants. Electrospray EP systems have been operated with ionic liquids and are the focus of this electric performance analysis. Specifically, this work presents a conceptual analysis of an electrospray thruster system that operates in or near the PIR on combustible ionic liquid propellant. A parametric investigation using judiciously bracketed figures is presented to study the effects of system parameters on thruster performance and mission capabilities.

A. Methods of Modeling Electrospray Propulsion

Traditional electrospray emission consists of fine droplets from a microjet that forms at the apex of an electrofluidic structure known as a Taylor cone [21]. This cone is formed from the application of a startup potential between a capillary containing a conducting fluid and an extractor grid downstream. Once formed, the applied voltage on the cone can be varied quite substantially, even to values below the startup potential. Excessive voltages can result in the deformation of the cone and multiple secondary emission points. A stable Taylor cone emits droplets and ions in proportions dependent on the flow rate of the propellant. A higher flow rate results in a predominant droplet emission, whereas a minimum flow rate yields a nearly PIR for some ionic liquids.

To quantify the performance of an electrospray propulsion system, two models of traditional solution-based sprays are initially investigated [21,22]. Both models are empirically based on a series of solutions consisting of a high dielectric constant solvent and a salt additive. They predict ISP, thrust, and droplet size based on a series of electrochemical properties and a proportionality curve between the emitted current and a dielectric constant. Unfortunately, these two models are invalid for use with ionic liquids. First, the two methods disagree on the functional form of the curve of the emitted current and dielectric constant. An analysis by Chen and Pui suggests that the results of this curve may depend greatly on the mobility of ions present in the fluid [23]. Since ionic liquids are typically composed of complex ions, the ion mobility of ionic liquids can be expected to differ significantly from the conventional additives of polar solvent solutions. Second, the typical values of the ionic liquid dielectric constant fall at the very edge of the range investigated in both models. Last, neither model is capable of predicting results near the PIR, which is the range of most interest here. Instead, in the following

sections, we outline a conceptual electrospray system and evaluate its performance and capabilities using ranges of parameters based on the current state of the art of electrospray and general EP technology.

B. Purely Ionic Regime Electrospray Conceptual Model

A future electrospray system that operates near the PIR consists of four main components: propellant with storage tank, propellant feed system, emitters, and power processing unit (PPU). Propellant from the storage tank is fed to the emitters, while spacecraft power is converted by the PPU and used to operate the emitters. A single emitter consists of a capillary containing the ionic fluid and either a single- or double-grid assembly. The grid closest to the capillary is the extraction grid and is required to provide the potential difference to form the Taylor cone and extract ions from the fluid. A second optional downstream grid can be used for enhanced control by providing acceleration or deceleration of the beam ions. The grid or set of grids can be operated with either fixed or alternating polarity. With fixed polarity operation, only one charged species is extracted (e.g., only positively charged ions), whereas with alternating polarity, both charge species are extracted, providing a net-neutral beam. This mode of operation may be desirable in future systems, because a net-neutral beam does not require a beam neutralizing device (e.g., a cathode). Because of the low thrust associated with each individual emitter, clusters of emitters are required to produce thrust levels of interest for future missions at low-power levels.

The following equations can be used to describe the electrospray system performance. Power supplied to the system can be related to thrust, ISP, and system efficiency using Eq. (4). The exit velocity of an ion that is accelerated through a net potential $\Delta\varphi$ is given by Eq. (5):

$$\eta_{\text{sys}} P_{\text{in}} = 1/2 \ \text{TI}_{\text{sp}} g_o \tag{4}$$

$$V_e = \sqrt{\frac{2e\Delta\varphi}{m}} \tag{5}$$

Results have shown that emission in the PIR consists of pure ions and ions traveling with clusters of N number of neutral pairs (the degree of solvation). To calculate thrust and ISP, the percentage of the mass flow rate that is pure ions and ions of various degrees of solvation is required [13]. This percentage can be determined from time-of-flight curves for ionic liquids that have operated near PIR. Such time-of-flight curves are produced experimentally by grounding the voltage to the emitter and measuring the current emitted as a function of time. The ions arrive at the collector in order of least to greatest mass (higher solvation). An examination of the curves shows that, typically, only the first two ion states ($N = 0, 1$) are present in the emission in any discernible quantity [13]. The ISP for a beam consisting of two species ($N = 0, 1$) is given by Eq. (6), where R_A is the percentage of the total flow that is pure ions, also known as the ion fraction:

Table 4 Ionic liquid anion, cation, and mass information

Property	HAN	BIMDCA
Anion	NO_3	C_2N_3
Cation	NH_3OH	$C_8H_{15}N_2$
Anion mass, g/mol	62	66
Cation mass, g/mol	34	139

$$I_{\text{sp}} = \frac{V_{e,N=0} R_A + V_{e,N=1}(1 - R_A)}{g_o} \tag{6}$$

The thrust of the system can be related to the total mass flow rate and ISP using Eq. (7). Finally, the mass flow rate of a single emitter can be related to the single emitter current and total mass flow rate using Eqs. (8) and (9):

$$T = \dot{m}_{\text{tot}} I_{\text{sp}} g_o \tag{7}$$

$$\dot{m}_{\text{tot}} = N_{\text{emit}} \dot{m}_{\text{emit}} \tag{8}$$

$$\dot{m}_{\text{emit}} = \frac{I_{\text{emit}} m}{e} \tag{9}$$

C. Purely Ionic Regime Electrospray Parametric Investigation

The electrospray model is used to investigate the effect of different parameters on system performance. Specifically, the effects of net accelerating voltage, system power, system efficiency, emitter current, and ion fraction on ISP, thrust, and the number of required emitters is investigated. From this analysis, conclusions regarding the most advantageous parameters for a future system are determined. Based on the chemical analysis presented previously, the two main ionic liquids focused on are HAN and BIMDCA, and their mass information is provided in Table 4.

The effect of net accelerating voltage on the ISP is shown in Fig. 3 for different beam ion fractions. These calculations assume that the electrospray system is operating in an alternating polarity mode with both positive (anion) and negative (cation) emission. Operation in a fixed polarity mode shifts the ISP slightly and is further discussed next. In the case of a single-grid emitter, the net accelerating voltage is the extraction voltage, whereas for a two-grid system, it is the combined fields of the extraction and acceleration/deceleration grids. For net accelerating voltages between 200 and 2000 V, the ISP varies from 1500 to 9000 s for HAN and 1000 to 6000 s for BIMDCA. For a fixed accelerating voltage and ion fraction, HAN always has a larger ISP than BIMDCA because it has a lower ion mass. Furthermore, these curves illustrate the effect of the ion fraction on ISPs. An ion fraction of one represents pure ion emission ($N = 0$), while a value of zero represents the emission of only the first solvated state ($N = 1$, an ion connected with a net-neutral anion–cation pair). For both HAN and BIMDCA, as the ion fraction decreases, the ISP decreases for

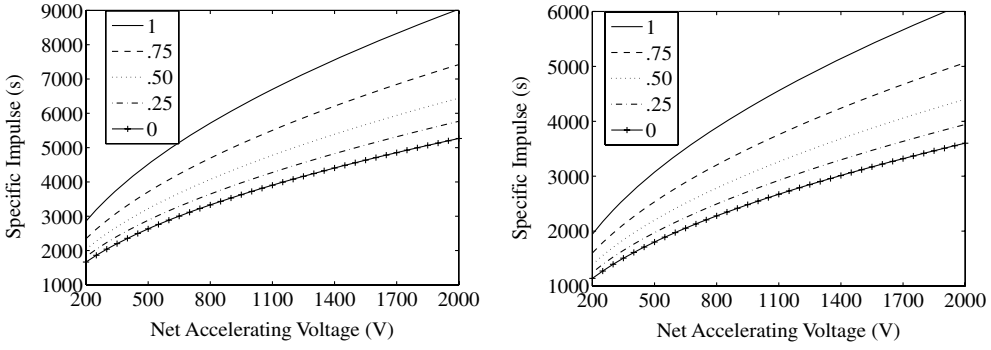

Fig. 3 The ISP as a function of net accelerating voltage for a) HAN and b) BIMDCA for different values of ion fraction.

fixed accelerating voltage. This is due to the fact that ions in the first solvated state are more massive than pure ions.

Operating the electrospray system in a fixed polarity mode, such that only anion or cation emission is achieved, slightly modifies the ISP from that shown in Fig. 3. For HAN, the ISP shifts, at most, $\pm 15\%$ with the increase corresponding to purely cation emission, while the shift for BIMDCA is $\pm 18\%$, with the increase corresponding to purely anion emission. Again, this result is due to the mass of the propellant ions that are extracted. In the alternating polarity mode, both the heavy (HAN anion and BIMDCA cation) and light (HAN cation and BIMDCA anion) ion species are extracted, yielding an averaged ISP. In fixed polarity mode, extraction of the heavier ion results in lower ISPs, while the lighter ion yields higher ISPs.

Thrust is plotted as a function of ISP for fixed input power and different levels of system efficiency in Fig. 4. The power level is set at 200 W, because missions that electrospray systems are being considered for are currently performed with low-power 200 W Hall thruster technology. Lower power levels reduce the thrust level according to Eq. (4), and the effect of power on electrospray system attributes is further investigated in the next section. For fixed ISPs, Fig. 4 shows that thrust decreases as efficiency decreases. Efficiencies of 75, 50, and 25% are investigated to provide a wide range of possibilities, since future electrospray system capabilities are still uncertain. However, the efficiency can still be bounded. System efficiency is not likely to be above 75%, since a single emitter is anticipated to have, at most, 85% efficiency [11], and current state-of-the-art EP power supplies are $\sim$90% efficient [24–26]. State-of-the-art Hall thruster systems are only $\sim$50% efficient [25–27] and, given the current level of immaturity of PIR electrospray technology, initial systems are likely to have even lower efficiency closer to 25%.

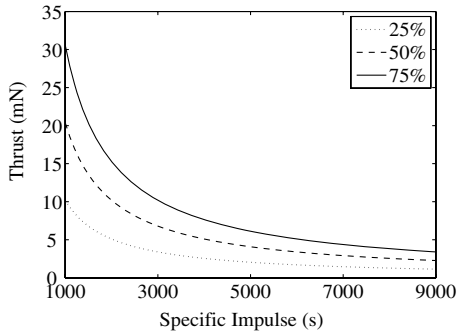

Fig. 4 Thrust versus ISP for different system efficiency values for 200 W of total power. Results are independent of propellant choice.

One of the major factors that impacts the future development of PIR electrospray technology for dual-mode propulsion applications is the large number of emitters required to achieve even low-thrust levels. Figure 5 shows how the number of required emitters changes with ISP, ion fraction, power, and the current each emitter is capable of emitting. These results are for a 200 W system. Individual emitter current levels of 1 nA, up to 1 μA, have been demonstrated [11], and we include 1 mA to show how a significant advancement in the technology might affect the system requirements. The number of emitters required is large, because the current, and thus the mass flow rate per emitter, is small. For instance, at the 2000 s ISP, a 200 W system with 50% efficiency has a thrust of 10.2 mN. Achieving this thrust requires a flow rate of 5.2×10^{-7} kg/s. If a single emitter only produces 1 μA of current, which is equivalent to 1.0×10^{-12} kg/s for PIR emission of HAN, then a total of 520,000 emitters are required. Figure 5a shows that the number of required emitters decreases as ISP increases because thrust and mass flow rate decrease for fixed power. The number of emitters for BIMDCA is 50% less than HAN, because BIMDCA is more massive, providing a larger flow rate per emitter. As the current per emitter increases, the number of required emitters decreases, because each emitter is capable of providing a higher flow rate and a larger portion of the thrust. If significant advances in the amount of current each emitter can provide are achieved, such that the current per emitter is as high as 1 mA, then the number of required emitters decreases to only a few hundred.

Figure 5b shows the effect of ion fraction on the number of required emitters. Results are shown for BIMDCA operating at

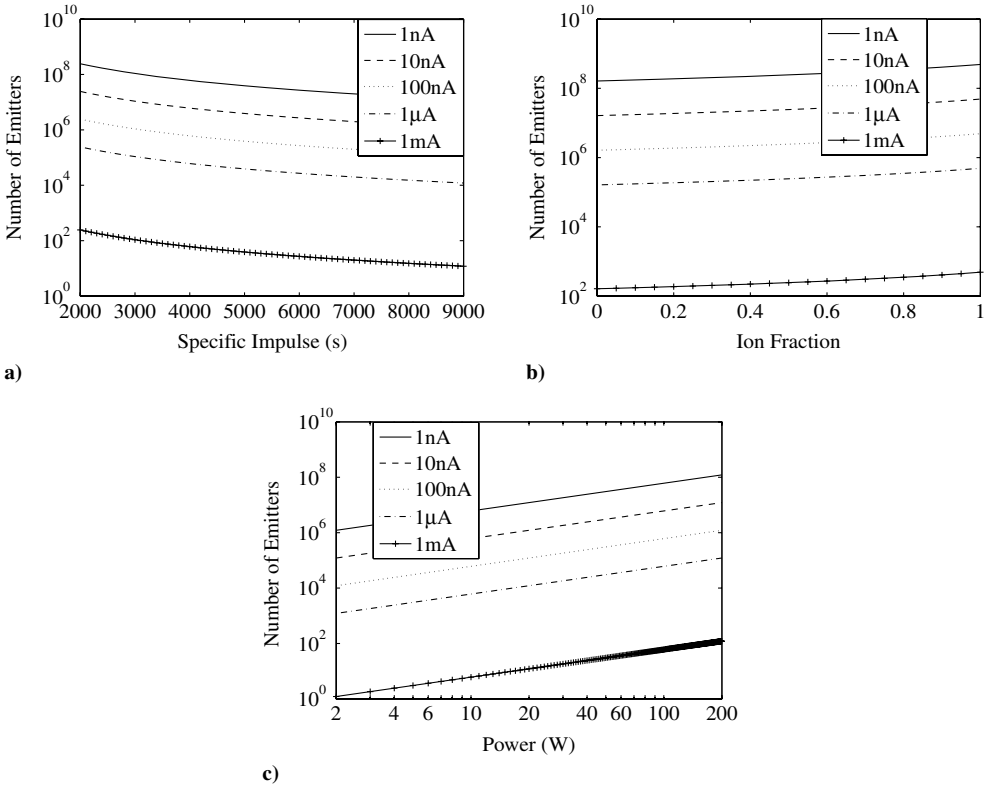

Fig. 5 Number of emitters versus a) ISP, b) ion fraction, and c) input power for BIMDCA.

200 W, 2000 s ISP, and 50% system efficiency. As the ion fraction decreases, the number of required emitters decreases, because the equivalent mass of the emitted ion increases, resulting in a larger mass flow rate per emitter. The trends are identical for HAN, with the number of emitters being 50% larger due to the smaller HAN ion mass. While the number of required emitters decreases with the ion fraction, even at an ion fraction of zero (only the $N = 1$ first solvated state being emitted), the number of required emitters for a 1 μA current per emitter is over 81,000. This is 66% less than the number of emitters required at an ion fraction of one, but it is still significant.

Figure 5c shows the effect of power on the number of required emitters. Results are shown for the 2000 s ISP, 25% system efficiency, and an ion fraction of 50%. As input power increases, the number of required emitters increases, because larger total flow rates are required to produce more thrust. At the 1 μA level, from 2 to 200 W, the number of emitters increases from 1200 to 12,000. Emitter capillaries vary in size, but typical diameters are 1–100 μm. If capillaries of a 10 μm inner diameter and a 100 μm outer diameter are spaced 50 μm apart, then 12,000 emitters would occupy a square with a side of length about 1.6 cm.

IV. Dual-Mode Benefits Trade Study

The following sections analyze the effect of dual-mode spacecraft propulsion capability on mission performance. Two main analytic investigations are performed. First, a combustible ionic liquid dual-mode propulsion system with a monopropellant chemical thruster and PIR electrospray system is studied. The effects of electrospray specific power, efficiency, and ISP are quantified in terms of the maximum changes in spacecraft velocity ΔV and thrust time. Results are presented as a function of the EP fraction: that is, the fraction of the total ΔV performed by the EP (electrospray) system. The second analysis compares the mission capabilities of five different spacecraft propulsion systems that have both a chemical and an electric thruster system. These propulsion systems include a combination of a conventional hydrazine monopropellant and a xenon Hall thruster, as well as a dual-mode ionic liquid monopropellant and electrospray system. The goal is to quantify the benefits of a dual-mode ionic liquid system over separate state-of-the-art chemical and electric systems. All of these analyses rely on a spacecraft systems mass budget that is described next.

A. Systems Mass Budgets

For all propulsion system configurations investigated, a mass budget is developed based on a 100 kg total spacecraft mass. In each case, a value of 35% of the total system mass is devoted to the propulsion system. For each configuration, the subcomponent masses are determined based on literature data and an approximation methodology [20,28,29]. Such estimates are necessary, because the amount of fuel available for each system varies based on the mass of its support hardware. For the conventional systems (e.g., combination of a hydrazine monopropellant and xenon Hall thruster), the total system mass is divided evenly between electrical and chemical propulsion subsystems.

Representative values for the mass of monopropellant, bipropellant, and Hall thrusters are obtained from literature in the range of the thruster performance being investigated [20,28,29]. Monopropellant and bipropellant thrusters have an average mass of 0.21 and 0.54 kg, respectively, with standard deviations of 0.09 and 0.18 kg. To ensure conservative estimates, the monopropellant and bipropellant thruster masses are estimated as 0.3 and 0.7 kg. Available literature did not indicate the mass of a BHT 200 Hall thruster, but the similarly sized SPT-50 has a mass of 0.8 kg [30]. Since the electrospray thruster is essentially a crucible with a lid consisting of emitters and an extraction grid, the mass is assumed to be at least half that of the Hall thruster. The data in the literature also provide the mass of the PPU for a Hall thruster [25,26]. Based on values reported for the NASA Solar Electric Propulsion Technology Application Readiness, the NASA Evolutionary Xenon Thruster, and SPT-50 PPU, the specific power is 161 W/kg, resulting in a PPU mass of 1.3 kg for a 200 W system.

Each main propulsion system also contains propellant tanks, pressurization tanks, feed lines, regulation valves, and mounting brackets. The masses of these subcomponents are determined using methodologies described by Humble et al. [31]. The propellant tank pressures are determined by starting with the specified chamber pressure of 300 psi and backing up through the propellant feed system. An injector head loss of 20% of the chamber pressure is assumed, along with overall line losses of 0.35 psi. The mass of each chemical propellant tank is calculated from the propellant storage pressure, the propellant volume (assuming a liquid incompressible state), and material properties [31]:

$$M_{\mathrm{ct}} = 6\frac{M_p \rho_m P_t}{\rho_p F_{\mathrm{tu}}} \tag{10}$$

The mass of the Hall thruster xenon propellant tank is computed assuming a maximum pressure of 1450 psi:

$$M_{\mathrm{et}} = 6\frac{V_{\mathrm{xe}} \rho_m P_t}{F_{\mathrm{tu}}} \tag{11}$$

Because of the high pressure, the volume of xenon is evaluated using the van der Waals equation of state in place of the ideal gas law [32].

A pumping system is required to maintain a constant propellant flow rate (due to the low mass of the system), and a pressure feed system is selected. Such a system must provide enough pressurant to occupy the volume of the entire main propulsion system at a pressure at least equal to the tank pressure. The pressurant tank pressure is limited to 1450 psi so that it is typical of spacecraft pressure vessels. When the pressure is limited, the mass of pressurant gas becomes coupled with the volume of the pressurant tank itself. Thus, an iterative procedure is used to compute both the mass of pressurant gas and the volume of the pressurant tank. The mass of the pressurant required to fill the main propulsion system is computed for an initial volume equal to that of the propellant tanks. The volume needed to store the pressurant is then computed. This new volume is added to the initial volume, and the total volume is used to calculate a new pressurant mass. This process is repeated until convergence, providing both pressurant mass and pressurization tank volume, and thus the pressurant tank mass.

The mass of lines and regulation valves are provided by the CPIA manual [20]. For typical monopropellant and bipropellant systems at the thrust level under consideration here, the mass of lines and valves combined would be approximately 50 and 90% of the thruster mass, respectively. Because of the high disparity between storage pressure and thruster pressure in EP systems, the valves and lines for the Hall thruster are assumed to have the same percent mass as those for the bipropellant thrusters. This value of 90% of the thruster mass is also assumed for the electrospray thruster because of the need for a high degree of mass flow control. Based on methods in literature, mounting brackets are assumed to be 10% of the total mass of the other components in the system [31]. Since the total mass of the main propulsion system is limited to 35 kg, all of these approximations are used in an iterative routine to find the distribution of system mass among the components. The results for each analysis are provided in the sections that follow.

B. Measure of System Performance

Measures of propulsion performance are based on the total change in velocity, mass of propellant consumed, and time required to produce the velocity change. All orbital perturbations are disregarded, as are potential gravity losses inherent in low-thrust applications. Therefore, the change in velocity reported here is ideal. Each of these metrics is computed as a function of the fraction of the total velocity change that is accomplished by EP; this is referred to as the EP fraction. For example, a value of 0 EP means that all change in velocity is accomplished by chemical means only, whereas 1 EP would mean that all change in velocity is accomplished by electrical means. To determine the total velocity change each system can produce, the rocket equation is used in a two-part form:

$$\Delta V = I_{\text{sp,chem}} g_o \ln(m_0/m_{f1}) + I_{\text{sp,elec}} g_o \ln(m_{f1}/m_{f2}) \qquad (12)$$

where the first term represents the change in velocity provided by chemical propulsion and the second term represents the change provided by EP. The values of satellite mass at the end of each subsequent burn (m_{f1} chemical thrust and m_{f2} electrical thrust) are restricted based on the available propellant mass. Furthermore, all chemical thrusting is assumed to take place before the electrical thrusting, and thrusting is continuous and not subject to specific orbital constraints. To determine the time required to apply the change in velocity, the mass flow rate of each thruster type is used in conjunction with the total mass of propellant consumed. The result is the sum of the chemical burn time and electric thrust time:

$$t = I_{\text{sp,chem}} g_o \frac{(m_0 - m_{f1})}{T_{\text{chem}}} + I_{\text{sp,elec}} g_o \frac{(m_{f1} - m_{f2})}{T_{\text{elec}}} \qquad (13)$$

C. Dual-Mode Ionic Liquid System

Mission performance of a dual-mode propelled spacecraft with an ionic liquid monopropellant thruster and PIR electrospray system is investigated in this section. The ionic liquid chemical thruster is assumed to have performance equivalent to 218 s ISP and 10 N thrust, which is typical for HAN ionic liquid thrusters [19]. The EP is a PIR electrospray, as described in Sec. III. Based on the previous analysis that showed higher powers are more desirable for stationkeeping and orbit transfer maneuvers, we assume an electric thruster input power of 200 W. The effects of electrospray specific power, system efficiency, and ISP on the mission performance are assessed in this section. Most results are presented as a function of EP fraction, which is the fraction of the total velocity change that is accomplished by the EP (electrospray) system.

Spacecraft propulsion system mass budget for a dual-mode ionic liquid system is shown in Fig. 6 as a function of electrospray specific power. Total available mass is 35 kg for the propulsion system. Values of specific power from 10 W/kg up to the EP state-of-the-art of about 150 W/kg are investigated. An increase in specific power means that less electrospray system mass is required to process the 200 W input power. As a result, PPU mass decreases,and propellant mass increases as specific power increases. The fraction of ionic liquid propellant available is 10.1 kg at a specific power of 10 W/kg, and it increases to 27.0 kg at 150 W/kg. PPU mass is larger than the propellant mass for specific power values below 12 W/kg. It has a mass of 19.6 kg at 10 W/kg and decreases to 0.93 kg at 150 W/kg. Thruster mass is the combined mass of the monopropellant thruster and electrospray emitters. Based on the system mass analysis described previously, these combine together for a 0.7 kg total mass and do not change with specific power. The mass fraction of other hardware associated with the propulsion system (valves, lines, tanks, and mounts) increases initially and then plateaus. Mass associated with these components is dependent on the mass of the propellant. For instance, as propellant mass increases, a larger tank, more pressurant, and a larger pressurant tank are required. All of these effects combine to slightly increase the mass of other required hardware. As specific power increases, other hardware mass plateaus at about 6.2 kg after 40 W/kg.

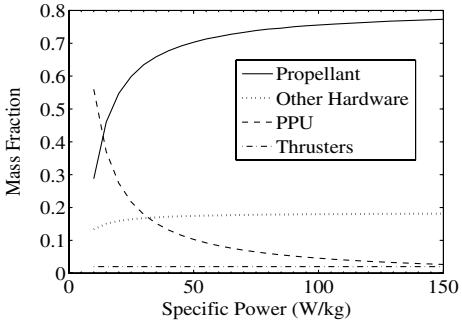

Fig. 6 Dual-mode ionic-liquid-propelled spacecraft propulsion system mass budget as a function of electrospray specific power.

The effects of specific power on the maximum possible change in spacecraft velocity and the required thrust time to accomplish that velocity change are shown in Fig. 7 as a function of the EP fraction. An EP fraction of zero means the ionic liquid monopropellant thruster provides all the change in velocity, while a fraction of one means the PIR electrospray system provides all the velocity change. These results are for a dual-mode system with an electrospray system ISP of 1000 s, 200 W input power, and 25% efficiency, yielding a thrust level of 10.2 mN from the analysis in Sec. III.

Figure 7a shows that the maximum possible change in spacecraft velocity is greatly affected by the fraction of EP used to complete the maneuver. Specifically, as EP fraction increases, the maximum ΔV increases. For a specific power of 10 W/kg, an EP fraction of zero has a maximum ΔV of 225 m/s, while an EP fraction of one has 1030 m/s. This trend is explained by the fact that, at an EP fraction of zero, the chemical thruster is completing all the ΔV with ISPs of only 218 s. At an EP fraction of one, the electrospray system completes all the ΔV with ISPs of 1000 s. At EP fractions between zero and one, a different fraction of the mission is performed with the chemical and electric systems, providing a ΔV between the extremes. Figure 7a also shows that, as specific power increases, maximum ΔV increases. However, the rate of increase in maximum ΔV decreases as specific power increases. This trend is explained by the results from Fig. 6, which show that, as specific power increases, the available propellant mass increases and plateaus. With more propellant mass, a spacecraft can accomplish a greater ΔV, regardless of the EP fraction.

Figure 7b shows that thrust time to accomplish the maximum change in velocity (Figure 7a) can vary from almost 0 to 300 days, depending on the EP fraction and electrospray specific power. For a specific power of 10 W/kg, at an EP fraction of zero, the thrust time is 36 min., while at an EP fraction of one, it is 111 days. As the EP fraction increases, the required thrust time increases, because the effective ISP increases as more EP is used. As specific power increases, the thrust time increases, because more propellant is available, and it takes a longer time to expend more propellant.

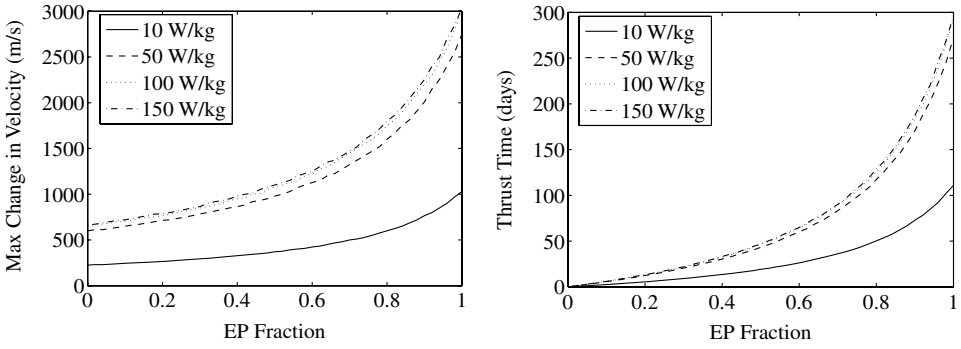

a) b)

Fig. 7 Effects of specific power on a) maximum spacecraft ΔV and b) required thrust time as a function of EP fraction.

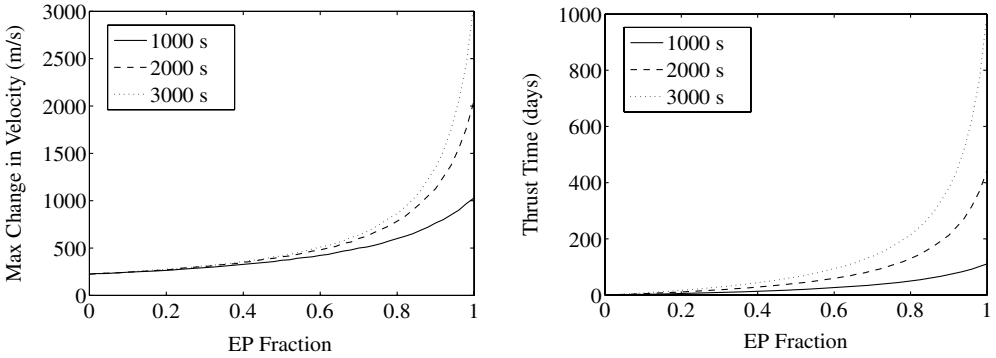

a) b)

Fig. 8 Electrospray ISP: a) maximum spacecraft ΔV and b) required thrust time as a function of EP fraction.

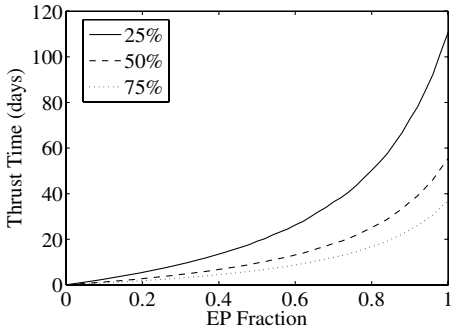

Fig. 9 Thrust time as a function of EP fraction for different electrospray system efficiency.

However, the rate of increase of thrust time decreases as specific power increases. Again, this trend is explained by the results from Fig. 6.

The ISP of the electrospray system is investigated in Fig. 8. The maximum spacecraft velocity change and thrust time are shown as a function of EP fraction for different values of the electrospray ISP. The electrospray system has 200 W input power, 25% efficiency, and a specific power of 10 W/kg. Figure 8a shows that higher ISPs provide larger ΔV, as expected. Furthermore, it shows that the benefit of higher ISPs is less pronounced as the EP fraction decreases. This is due to the fact that, as the EP fraction decreases, less ΔV is being provided by the electrospray system. For instance, the maximum ΔV for a 2000 s operation becomes 20% larger than operation at 1000 s, only for an EP fraction greater than 70%. Comparison of the ΔV between 3000 and 2000 s ISP shows that 3000 s operation is 20% larger than that at 2000 s for an EP fraction greater than 90%. Figure 8b shows that ISP has a greater effect on thrust time at larger EP fraction.

Electrospray system efficiency effects on the dual-mode ionic-liquid-propelled spacecraft are examined in Fig. 9. These results are for a specific power of 10 W/kg and ISPs of 1000 s. Changes in electrospray system efficiency have no effect on the maximum possible change in spacecraft velocity, because the total available propellant mass and the system ISP are not affected by efficiency in this model. However, system efficiency does affect the required thrust time. As Fig. 9 shows, as the EP fraction increases, thrust time increases for fixed efficiency. This is explained by the fact that, as EP fraction increases, a larger portion of the ΔV is performed by the low-thrust electrospray system, such that a longer thrust time is required. Figure 9 also shows that, as efficiency decreases, the thrust time increases. For fixed input power and fixed ISP, as efficiency decreases, thrust decreases (Fig. 4). To expend the same amount of propellant at a lower thrust, a longer thrust time is required.

Based on the analysis presented in this section, several conclusions can be drawn regarding an ionic liquid dual-mode propulsion system. Specific power is important for decreasing PPU mass and increasing propellant mass. However, as Fig. 6 shows, the benefit decreases as specific power increases. Specifically, increasing specific power above about 50 W/kg no longer provides substantial benefits. This same trend is again evident in Fig. 7 for the maximum change in spacecraft velocity and thrust time. The electrospray ISP has a dramatic effect on maximum ΔV and thrust time, but only for EP fractions close to one. Operation of the electrospray system with ISPs greater than about 2000 s yields thrust times greater than 14 months to expend all the propellant. These thrust times are greater than desired for the types of dual-mode missions envisioned.

D. Comparison of Dual-Mode with Current Technology

This section compares the mission performance of three candidate dual-mode propulsion systems and two conventional propulsion systems. A conventional propulsion system is defined as having a traditional mono- or bipropellant thruster and an EP system (xenon Hall thruster) that do not use the same propellant. A dual-mode system is a mono- or bipropellant thruster and an EP system (electrospray) that both use at least one common propellant. A description of each propulsion system combination and its performance are described in the next section, along with a mass analysis. The maximum spacecraft velocity change and thrust time for each combination are described in the Sec. IV.D.2. Finally, the different

Table 5 Propulsion system performance specifications

System	1	2	3	4	5
			Chemical Mode		
Propellant	N_2H_4	N_2H_4/NTO	BIMDCA/NTO	BIMDCA/HAN	HAN
ISP, s	227	270	239	267	218
Thrust, N	10	10	10	10	10
Mass flow, g/s	4.4	3.7	4.2	3.7	4.6
Type	Monopropellant	Bipropellant	Bipropellant	Bipropellant	Monopropellant
			Electric Mode		
Propellant	Xenon	Xenon	BIMDCA	BIMDCA/HAN	HAN
ISP, s	1390	1390	1600	1900	2300
Thrust, mN	12.8	12.8	6.4	5.4	4.4
Mass flow, mg/s	0.94	0.94	0.41	0.46	0.20
Type	Hall	Hall	Electrospray	Electrospray	Electrospray

Table 6 Mass budget breakdown for all systems

System	1	2	3	4	5
Thruster, kg	1.10	1.50	1.10	1.10	0.70
Fuel, kg	14.1	7.31	5.11	5.32	9.96
Oxidizer, kg	0.00	6.10	4.25	4.09	0.00
Pressurant, kg	0.60	0.50	0.34	0.32	0.41
Fuel tank, kg	0.37	0.19	0.13	0.13	0.25
Oxidizer tank, kg	0.00	0.11	0.08	0.06	0.00
Pressurant tank, kg	0.47	0.39	0.27	0.25	0.32
Lines/valves, kg	0.87	1.35	0.99	0.99	0.63
Xenon, kg	12.3	12.3	0.00	0.00	0.00
Xenon tank, kg	0.82	0.82	0.00	0.00	0.00
PPU, kg	1.33	1.33	19.6	19.6	19.6
Structural mounts, kg	3.19	3.19	3.19	3.19	3.19
Summary					
Chemical propellant, kg	14.1	13.4	4.25	0.00	0.00
Electric propellant, kg	12.3	12.3	0.00	0.00	0.00
Common propellant, kg	0.00	0.00	5.11	9.41	9.96
Other hardware, kg	8.69	9.34	25.6	25.6	25.0

combinations are compared with each other to quantify performance and system requirements for future dual-mode propulsion.

1. *Systems Performance and Mass Budgets*

Table 5 lists the performance specifications for the five propulsion system combinations investigated. Systems 1 and 2 are typical onorbit propulsion systems that use hydrazine and NTO in conjunction with a Hall thruster and are termed conventional. The purpose of system 3 is to bridge the gap between completely conventional and pure dual mode by using the same fuel in both chemical and electric modes, but using the conventional oxidizer NTO for chemical propulsion only. System 4 represents a pure dual-mode propulsion system that uses a combination of ionic liquid HAN and BIMDCA to accomplish both chemical and EP. A HAN monopropellant chemical thruster and an electrospray thruster makes system 5 a dual-mode system. System 5 is the type of system investigated in the previous section.

Chemical propulsion performance for these five systems is determined based on the previous analysis (see Table 2) and typical performance for these propellants [19]. The EP systems are all assumed to have 200 W input power. The Xenon Hall thruster performance presented in Table 5 is typical of a 200 W BHT-200 device [27]. For the ionic liquid electrospray systems, a 200 V net accelerating potential and 50% ion fraction are assumed with ISPs (given by Fig. 3). The efficiency of the system is likely to be low due to the PPU and the substantial deceleration of extracted ions, so an efficiency of 25% is assumed. At the mass flow rate levels shown in Table 5, approximately 200,000 emitters are required if a single emitter provides 1 μA of current. The combined BIMDCA/HAN electrospray system ISP is set at the mass-averaged ISP based on the propellant masses found in the next section. The effect of changing these electrospray system parameters was investigated and described in the previous section. Other values can be used for the calculations and, as the technology develops, better assumptions and estimations will be available. Given the current incipient state of the art, the purpose of this analysis is to compare systems that consist of conventional propulsion and true dual-mode capability in an effort to quantify the potential benefits and system requirements for a dual-mode system.

A mass analysis is completed for each of the five combinations and is shown in Table 6. The procedure was described previously in Sec. IV.A. For 200 W electrospray systems, we assume a specific power of 10 W/kg. The result is that systems 3, 4, and 5 have a PPU mass of 19.6 kg and an electrospray thruster mass of 0.4 kg. As shown in the table, the PPU mass dominates the mass budget for the dual-mode electrospray configurations. The effects of higher specific power are analyzed and described in the previous section. Those results and the analysis presented next are used to draw conclusions regarding requirements for future dual-mode systems that use PIR electrospray systems.

2. *Trade Study Results*

Figures 10 and 11 show the results for systems 1 and 5, respectively. Results for these two systems are shown and discussed in detail, whereas results for systems 2, 3, and 4 are not shown but are also discussed. Figure 10 shows the results for system 1. This is the

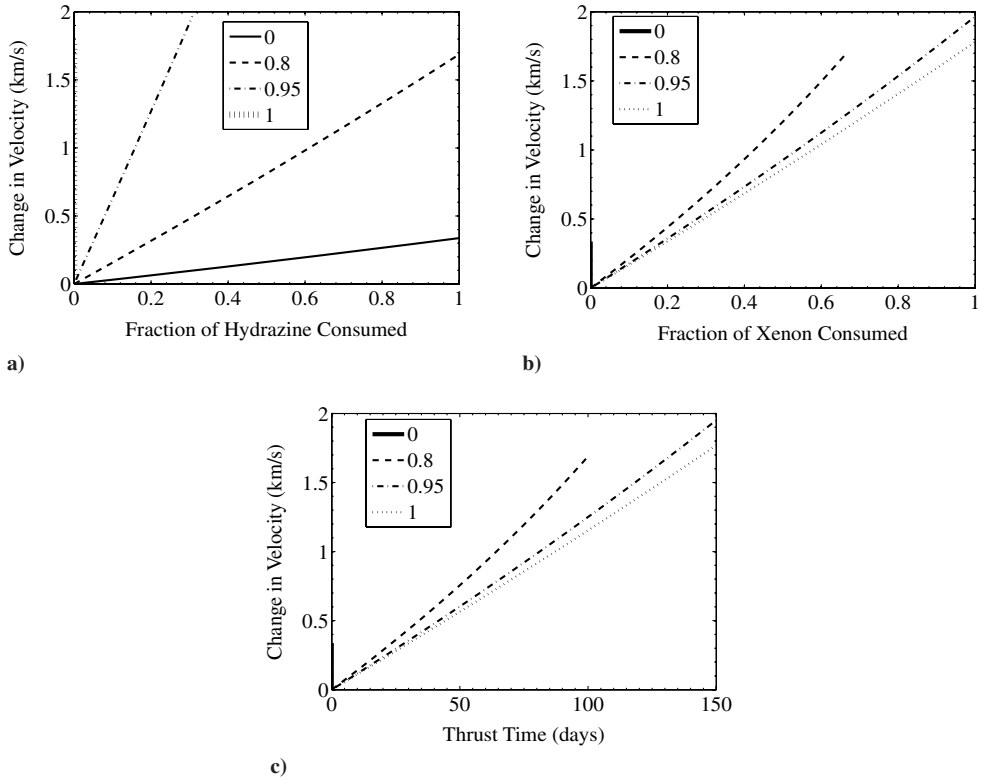

Fig. 10 System 1 performance for lines of constant EP fraction.

hydrazine monopropellant and Hall thruster configuration. Figure 10a shows the fraction of hydrazine consumed as a function of the change in spacecraft velocity for different values of an EP fraction. At 0 EP, a maximum velocity change of 370 m/s is obtained, and all of the hydrazine is consumed. At 0.86 EP, the maximum velocity of the system transitions from being limited by chemical propellant to being limited by electric propellant. Increasing the EP fraction beyond this point leaves unused chemical propellant in the tank, thus incurring a mass penalty for accelerating the chemical propellant; if the fuel is not burned, the potential change in velocity is not realized. For example, in Fig. 10a, operating at 0.95 EP achieves higher change in velocity than at an EP fraction of one. For the 0.95 EP case, 30% of the hydrazine is used, whereas at 1 EP, all of the hydrazine remains. Thus, at 0.95 EP, the spacecraft has less mass to accelerate when the electric mode is used. Operating with an EP fraction of one results in no consumption of hydrazine fuel. Chemical propellant remains in the tank after 0.86 EP, because there is insufficient electric propellant to produce a higher change in velocity. In the region from 0.86 to 1 EP, electric propellant is the limiting factor in the change in velocity.

Figure 10b shows the fraction of xenon propellant consumed as a function of the change in spacecraft velocity for different values of an EP fraction, these results correspond with Fig. 10a. At 0 EP, no xenon propellant is consumed. As an EP fraction increases, the fraction of xenon propellant consumed increases. At an EP fraction of one, the maximum velocity obtained is 1780 m/s. However, this is not the maximum velocity that the system can produce. The maximum velocity of 2249 m/s occurs at the point of transition of 0.86 EP. For values of EP lower than 0.86, the chemical propellant is the limiting factor in change in velocity, and electric propellant remains in the tank.

Figure 10c shows the time required to obtain a specific change in velocity for different values of an EP fraction. At 0 EP, the time required to accomplish the maximum change in velocity is only 52 min. As an EP fraction increases, the time required to perform the change in velocity increases until it reaches 150 days. The maximum velocity change at 0.86 EP also takes approximately 150 days.

Figure 11 shows the results for system 5. This is the HAN monopropellant and electrospray configuration. Figure 11a shows the fraction of HAN consumed as a function of the change in spacecraft velocity for different values of an EP fraction. Regardless of the EP fraction, all of the propellant can be consumed, unlike the results from system 1, where some propellant may be left over after maximum velocity change is achieved. Because this is a dual-mode system with common propellant, only one chart is required to describe the propellant consumption trends. At 0 EP, the maximum velocity achieved is 224 m/s. As an EP fraction increases, the maximum velocity possible increases, and the curve rotates upward. The maximum velocity for system 5 is 2350 m/s and occurs at an EP fraction of one. The use of common propellant means no point of transition exists as in the case of system 1. Instead, the maximum velocity occurs when propellant is used completely as electric propellant.

Figure 11b shows the time required to obtain the change in velocity for different values of an EP fraction. At 0 EP, the time required to perform the maximum velocity change is only 35 min. This is 67% of the time required by system 1 because both systems have a thrust of 10 N, but system 5 has only 70% of the available chemical propellant of system 1. Because system 5 has an electrospray thruster with ISPs greater than the Hall thruster of system 1, it requires about 1.5 years to accomplish the maximum change in velocity.

In the case of system 2, hydrazine is used in a bipropellant system paired with NTO, and a Hall thruster is used for EP. By using a bipropellant thruster, a change in velocity of 400 m/s is possible at 0 EP. This results in complete consumption of both hydrazine and NTO propellants. As the fraction of EP is increased, the fraction of NTO and hydrazine consumed are identical because they are directly related through the equivalence ratio. The same transition from chemical-propellant-limited to electric-propellant-limited maximum velocity that is observed in system 1 also occurs for system 2; in the case of system 2, it occurs at 0.85 EP. At this point, the maximum velocity is 2460 m/s. Because of the increased dry mass of system 2, it produces only a 2% greater change in velocity despite having ISPs 19% greater than system 1. The Hall thruster is burdened by the extra dry mass of the bipropellant system, resulting in a decrease in system acceleration. As with the case of system 1, any increase in an EP fraction results in higher xenon consumption. A decrease in chemical propellant consumption only occurs after the transition point. At 0 EP, system 2 requires 59 min. for maximum change in velocity. As with all systems, an increase in an EP fraction results in longer thrust duration. Similar to system 1, performing maximum change in velocity at the transition point requires 150 days.

For system 3, the ionic liquid BIMDCA is substituted for hydrazine in the bipropellant thruster: NTO is maintained as the oxidizer. In place of a Hall thruster, an electrospray thruster is used, also operating on BIMDCA. At 0 EP, system 3 is capable of producing a velocity change of 230 m/s. System 3 obtains a maximum velocity change of 823 m/s at an EP fraction of one. At all EP fractions, all of the BIMDCA is consumed. However, as the EP fraction increases, greater amounts of the NTO remain unused until, at an EP fraction of one, all of the NTO remains in the tank. The extra oxidizer mass decreases performance, and it is probably best ventilated in proportion to the amount of BIMDCA consumed. Ventilation of some NTO would leave the system capable of performing the maximum chemical change in velocity while increasing EP performance because of reduced system mass. The penalty is that the oxidizer is put into orbit with the spacecraft and now provides no gain in overall system performance. At 0 EP, 37 min. are required to perform the maximum velocity change. At an EP fraction of one, 145 days are required to produce a maximum change in velocity.

For system 4, BIMDCA is retained as the bipropellant fuel, but the oxidizer HAN is used in place of NTO. At 0 EP, the maximum velocity change possible is 260 m/s: all of the BIMDCA and HAN propellants are consumed. For all EP fractions, all propellants are consumed. By augmenting the electrospray of BIMDCA with higher ISP HAN, a maximum velocity of 1840 m/s is obtained for an EP

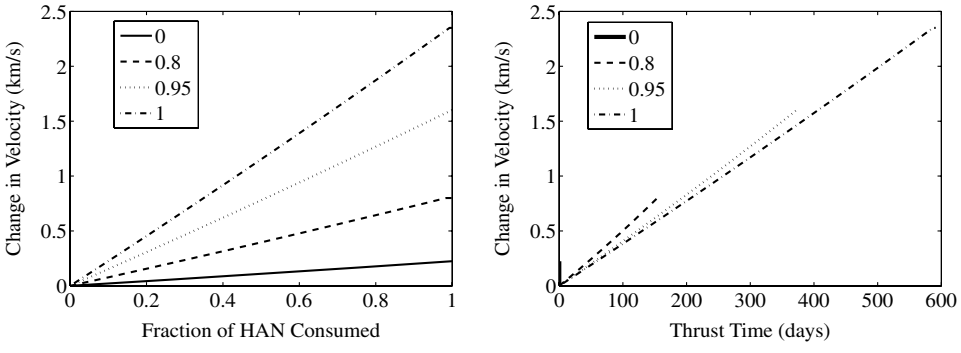

a) b)

Fig. 11 System 5 performance for lines of constant EP fraction.

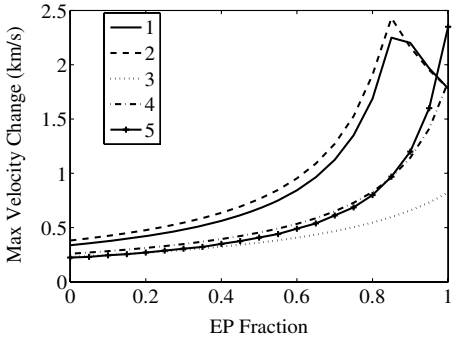

Fig. 12 Maximum change in velocity versus EP fraction for systems 1–5.

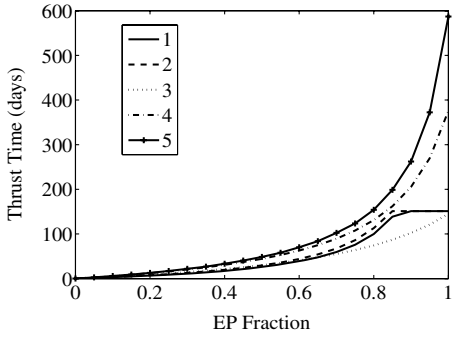

Fig. 14 Total time required to accomplish maximum change in velocity versus EP fraction for systems 1–5.

fraction of one. As with all systems, an increase in EP fraction results in longer thrust duration. At 0 EP, 41 min. is required for maximum velocity change. This increases to 1 yr for the case of 1 EP.

3. Trade Study Analysis

Figure 12 presents a comparison of the maximum change in velocity for each of the five systems. It is evident that the performances of systems 1 and 2 are virtually identical for small changes in velocity, with a small advantage for system 2 at an EP fraction of less than 0.85. The performance of systems 1 and 2 becomes effectively identical when the xenon propellant becomes the limiting factor in the maximum velocity change for both systems (occurring at 0.86 and 0.85 EP, respectively). Initially, both bipropellant systems 3 and 4 outperform the monopropellant system 5 in maximum velocity change. This is expected because of the increase in chemical ISP performance for the bipropellant systems. The higher ISP of the EP for system 5 overtakes that of system 3 at 0.25 EP. System 5 does not surpass the performance of system 4 until it reaches above 0.82 EP. Systems 3, 4, and 5 are the dual-mode systems and, for the assumed propulsion and system capabilities, they all provide a lower maximum velocity than the conventional systems for all EP fractions.

Figure 12 illustrates the importance of specific power for a dual-mode ionic liquid propulsion system to be competitive with conventional technology. The dual-mode systems 3, 4, and 5 are unable to provide the same maximum change in spacecraft velocity as the conventional systems 1 and 2. This result is due to the power supply penalty. For the 200-W 25% efficiency electrospray systems assumed here, a specific power of 10 W/kg requires a 19.6 kg PPU that accounts for over 50% of the allowed propulsion system mass. There simply is not enough mass left for propellant. Increasing efficiency provides more thrust to reduce trip time, but it does not affect maximum spacecraft velocity (Fig. 11). Current state-of-the-art colloid systems have a specific power of 1 W/kg [33]. As shown in Fig. 7, increasing specific power within the 10–50 W/kg range has a profound impact on the maximum possible velocity change. Because a dual-mode system makes use of common propellants and tanks, the specific power does not need to be as high as current Hall thruster technology (∼150 W/kg). However, based on the calculations and investigation presented here, a future ionic liquid electrospray system must have a specific power of at least 15 W/kg to compete with conventional hydrazine and Hall thruster technology. It is also important to note that, even if specific power remains low, in some mission scenarios, the onorbit flexibility of a dual-mode system may outweigh the penalty in total impulse.

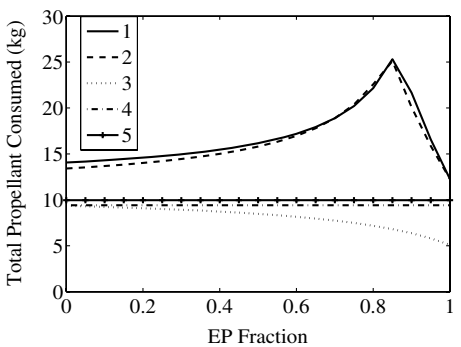

Fig. 13 Total propellant mass expended for maximum change in velocity versus EP fraction for all systems.

Figure 13 shows the total propellant expended for the maximum change in velocity shown in Fig. 12. Examination of systems 4 and 5 in Fig. 13 shows that a dual-mode system offers the advantage that, under any thrusting condition, all propellant is consumed. System 3 initially consumes all of the BIMDCA and NTO propellants, but as the EP fraction is increased, the amount consumed decreases because of the residual NTO oxidizer. Starting at around 0.75 EP, systems 1 and 2 show an interesting exchange in the propellant mass consumed. At this point, the bipropellant system 2 consumes more propellant than system 1 because of the larger amount of chemical propellant present in system 1. At each EP fraction, until the systems reach their respective transition points, all chemical propellant is expended. As a result, when system 2 begins its electrical thrusting, it has a higher dry mass to accelerate. This extra mass requires additional xenon propellant to affect the EP fraction of the total change in velocity, thus resulting in higher propellant use. This effect ceases almost immediately after the xenon propellant becomes the limiting factor in the maximum velocity. In the region, from an EP fraction of 0.85 to 1, system 1 consumes more propellant mass than system 2 because, now, less of the chemical propellant is consumed. This leaves additional mass for the EP system to accelerate, resulting in a higher consumption of xenon, and thus a higher total propellant mass consumption.

Figure 14 shows that the improved propellant savings associated with a higher EP fraction comes at the cost of mission time. Maneuvers taking hundreds of days are required to reach a maximum change in velocity. In the case of conventional systems (1 and 2), a plateau in mission time is observed, because once the maximum change in velocity accomplished by EP is reached for both systems, the systems are already thrusting for as long as possible. After this point, the few hours required to fire the chemical systems are insignificant in comparison to the 150 days to expel the xenon propellant, resulting in the effective plateau. Because of the higher ISP of the electrospray system, the dual-mode systems (3, 4, and 5) have higher thrust durations, even though the quantity of propellant is reduced for these systems.

V. Conclusions

A class of propellants known as ionic liquids is identified that can be used in both chemical and electric modes of propulsion. Based on CEA simulations of bipropellant combustion, the ionic liquid fuel and oxidizer combinations investigated are comparable to existing space storable propellants with differences on the order of a few percent. A comparison of the predicted ISPs of ionic liquids with hydrazine and UDMH shows that ionic liquid fuels have 3–12% lower ISPs when paired with NTO oxidizer. However, when paired with HAN oxidizer, the ISP of the ionic liquids is 1–4% lower than that of hydrazine and UDMH paired with NTO. Ionic liquids are also

attractive propellants because of their high density. Results indicate that ionic liquids can have up to a 40% greater density impulse (the product of density and ISP), signifying greater storability, which makes them attractive as space storable propellants.

An electrospray EP system may be capable of operating with ionic liquid propellant in the pure ion emission regime. For HAN and BIMDCA, voltage levels required for extraction of ions from these liquids (greater than 1000 V) cause acceleration that results in very high ISPs ($\sim$4000–6000 s). To reduce the ISP to levels envisioned for orbit raising and stationkeeping ($\sim$1000–2000 s), future ionic liquid electrospray systems require either a deceleration grid or propellant ions with higher mass [i.e., lower ion fraction or higher solvated state ($N > 0, 1$)]. In addition, higher emission current per electrospray emitter is desirable for future systems. Even at low power ($\sim$10–100 W), higher current emission (>1 μA per emitter) is required to reduce the total number of required emitters. Ten or even hundreds of thousands of emitters are required for an electrospray system at these power levels, so microfabrication processes are imperative for fabrication of electrospray emitter arrays.

Microfabrication of large emitter arrays is likely possible with current technology. During early testing and development of colloid electrospray devices, the area of microfabrication was still in its infancy. As a result, alternative capillary and device geometries were required to increase the current per emitter. Since then, the microfabrication, and even nanofabrication, industry has grown to permeate almost all areas of engineering technology and continues to expand based on ever increasing requirements. Current fabrication technology is capable of fabricating emitter arrays for obtaining almost every possible thrust level desired from an EP system. In fact, there are designs being investigated that focus on developing the electrospray thruster, such that it becomes the standard for future space propulsion technology [34–36].

The EP part of a dual-mode system has a significant effect on spacecraft performance capability. Specific power is perhaps the most important quantity, because it determines the EP system mass requirements and the mass remaining that is available for propellant. Increasing specific power from 10 to 50 W/kg can provide almost two times more ΔV at an EP fraction of one and three times more at an EP fraction of zero, where the EP fraction is the percentage of the ΔV completed by the EP system. EP ISP should be within the $\sim$1000–2000 s range so that thrust levels are high enough to provide a realistic trip time on the order of a few 100 days. Electrospray system efficiency is likely to be low for first-generation devices that may require deceleration grids and alternating polarity. Low efficiency reduces thrust and causes thrust time to increase.

Results also indicate that the EP part of a dual-mode system determines overall feasibility and advantages over conventional technology. Specifically, increasing specific power of an electrospray system from the current state-of-the-art 1 W/kg [33] up to at least 10 W/kg is mandatory for these systems to be considered for orbit-raising-type and stationkeeping-type maneuvers for micro- and medium-sized satellites. In fact, based on our calculations, a specific power of 15 W/kg is required to compete with current state-of-the-art hydrazine monopropellant and xenon Hall thruster technology. In other words, if electrospray specific power is less than 15 W/kg, our analysis indicates that the combination of a hydrazine monopropellant and a xenon Hall thruster can provide larger total impulse to a spacecraft in a shorter amount of time.

If specific power as high as 15 W/kg is not possible, the use of a dual-mode system may still have other mission benefits due to its flexible thrust history. The growing threat of orbit debris offers a great opportunity for dual-mode systems. Their flexibility may permit an asset to respond quickly to an imminent hazard using a primarily chemical maneuver and slowly return to its original orbit using higher efficiency EP as the threat subsides. On the other hand, if no threat is encountered, the system may provide long-term orbit maintenance capability. In the fast-paced world of military conflict, such systems are ideal for rapid deployment of space assets. With little knowledge of the thrust history before deployment, a generic spacecraft may have a thrust history that is dictated as the mission evolves rather than before launch. The concepts of orbital refueling and space tugs may also benefit from a dual-mode propulsion system; sharing a common propellant means both the tug and the assets being transported or refueled will operate on the same propellant.

Acknowledgments

The authors acknowledge the financial support of the Missouri Space Grant Consortium in the preliminary chemical propulsion work and the advice and encouragement of the members of U. S. Air Force Research Laboratory, Edwards Air Force Base. The authors would like to thank U. Koylu, D. Riggins, and P. Reddy of the Missouri University of Science and Technology for their advice throughout this investigation. All members of the Aerospace Plasma Lab at the University of Missouri Science and Technology are also acknowledged for many fruitful discussions.

References

[1] Lide, D. R., *CRC Handbook of Chemistry and Physics*, 88th ed., Taylor and Francis Group, Philadelphia, 2008, pp. 6.153–6.156.

[2] Zube, D., Wucherer, E., and Reed, B., "Evaluation of HAN-Based Propellant Blends," 39th AIAA Joint Propulsion Conference, AIAA Paper 2003-4643, 2003.

[3] Boatz, J., Gordon, M., Voth, G., and Hammes-Schiffer, S., "Design of Energetic Ionic Liquids," *DoD HPCMP Users Group Conference*, IEEE Publ., Piscataway, NJ, Pittsburgh, 2008, pp. 196–200.

[4] Smiglak, M., Reichert, M. W., Holbrey, J. D., Wilkes, J. S., Sun, L., Thrasher, J. S., Kirichenko, K., Singh, S., Katritzky, A. R., and Rogers, R. D., "Combustible Ionic Liquids by Design: Is Laboratory Safety Another Ionic Liquid Myth?," *Chemical Communications (Cambridge)*, No. 24, 2006, pp. 2554–2556. doi:10.1039/b602086k

[5] Amariei, D., Courtheoux, L., Rossignol, S., Batonneau, Y., Kappenstein, C., Ford, M., and Pillet, N., "Influence of the Fuel on the Thermal and Catalytic Decompositions of Ionic Liquid Monopropellants," 41st AIAA Joint Propulsion Conference, AIAA Paper 2005-3980, 2005.

[6] Chang, Y., and Kuo, K., "Assessment of Combustion Characteristics and Mechanism of a HAN-Based Liquid Monopropellant," 37th Joint Propulsion Conference, AIAA Paper 2001-3272, 2001.

[7] Meng, M., Khare, P., Risha, G., Yetter, R., and Yang, V., "Decomposition and Ignition of HAN-Based Monopropellants by Electrolysis," 47th AIAA Aerospace Sciences Meeting, AIAA Paper 2009-451, 2009.

[8] Schneider, S., Hawkins, T., Rosander, M., Vaghjiani, G., Chambreau, S., and Drake, G., "Ionic Liquids as Hypergolic Fuels," *Energy and Fuels*, Vol. 22, No. 4, June 2008, pp. 2871–2872. doi:10.1021/ef800286b

[9] Gao, H., Joo, Y., Twamley, B., and Shreeve, J., "Hypergolic Ionic Liquids with 2-2, Dialkyltiazanium Cation," *Chemistry international*, Vol. 121, No. 15, March 2009, pp. 2830–2833. doi:10.1002/ange.200900094

[10] Dambach, E., Heister, S., Ismail, I., Schneider, S., and Hawkins, T., "An Investigation into the Hypergolicity of Dicyanamide-Based Ionic Liquid Fuels with Common Oxidizers," *JANNAF 4th Propulsion Meeting*, Orlando, FL, 2008.

[11] Lozano, P., and Sanchez, M., "Efficiency Estimation of EMI-BF4 Ionic Liquid Thrusters," 41st AIAA Joint Propulsion Conference, AIAA Paper 2005-4388, 2005.

[12] Lozano, P., Glass, P., and Sanchez, M., "Performance Characteristics of a Linear Ionic Liquid Electrospray Thruster," *29th International Electric Propulsion Conference*, IEPC Paper 2005-0192, 2005.

[13] Garoz, D., Bueno, C., Larriba, C., Castro, C., and Fernández de la Mora, J., "Taylor Cones of Ionic Liquids from Capillary Tubes as Sources of Pure Ions for Electrical Propulsion," 42th AIAA Joint Propulsion Conference, AIAA Paper 2003-4846, 2006.

[14] Dominick, S., "Design, Development, and Flight Performance of the Mars Global Surveyor Propulsion System," 35th AIAA Joint Propulsion Conference, AIAA Paper 1999-2176, 1999.

[15] Gordon, S., "Computer Program for Calculation of Complex Chemical Equilibrium Compositions and Applications," NASA RP-1311-P2, 1996.

[16] Emel'yanenko, V., Verevkin, S. P., and Heintz, A., "The Gaseous Enthalpy of Formation of the Ionic Liquid 1-Butyl-3-Methylimidazolium Dicyanamide from Combustion Calorimetry, Vapor Pressure Measurements, and Ab Initio Calculations," *Journal of the American*

Chemical Society, Vol. 129, No. 13, March 2007, pp. 3930–3937. doi:10.1021/ja0679174

[17] Emel'yanenko, V., Verevkin, S. P., Heintz, A., Corfield, J., Deyko, A., Lovelock, K. R. J., Licence, P., and Jones, R. G., "Pyrrolidinium-Based Ionic Liquids.1-Butyl-3-Methylpyrrolidinium Dicyanamide: Thermochemical Measurement, Mass Spectrometry, and Ab Initio Calculations," *Journal of Physical Chemistry B*, Vol. 112, No. 37, Aug. 2008, pp. 11,734–11,742. doi:10.1021/jp803238t

[18] Tao, G., Guo, Y., Joo, Y., Twamley, B., and Shreeve, J., "Energetic Nitrogen-Rich Salts and Ionic Liquids: 5-Aminotetrazole (AT) as a Weak Acid," *Journal of Materials Chemistry*, Vol. 18, No. 45, Oct. 2008, pp. 5524–5530. doi:10.1039/b811506k

[19] Sutton, G. P., and Biblarz, O., *Rocket Propulsion Elements*, 7th ed., Wiley–Interscience, New York, 2001, pp. 45–101, 160–361.

[20] "CPIA/M5 Liquid Propellant Engine Manual," Johns Hopkins Univ. Chemical Propulsion Information Agency, Columbia, MD, 1998.

[21] Fernández De La Mora, J., and Loscertales, G., "The Current Emitted by Highly Conducting Taylor Cones," *Journal of Fluid Mechanics*, Vol. 260, 1994, pp. 155–184. doi:10.1017/S0022112094003472

[22] Ganan-Calvo, A. M., "The Size and Charge of Droplets in the Electrospraying of Polar Liquids in Cone-jet mode, and the Minimum Droplet Size," *Journal of Aerosol Science*, Vol. 28, No. 2, March 1997, pp. 249–275. doi:10.1016/S0021-8502(96)00433-8

[23] Chen, D., and Pui, D., "Experimental Investigation of Scaling Laws for Electrospraying: Dielectric Constant Effect," *Aerosol Science and Technology*, Vol. 27, No. 3, Sept. 1997, pp. 367–380. doi:10.1080/02786829708965479

[24] Pencil, E. J., "Recent Electric Propulsion Development Activities for NASA Science Missions," *IEEE Aerospace Conference*, IEEE Publ., Piscataway, NJ, March 2009.

[25] Pinero, L. R., Hopson, M., Todd, P. C., and Wong, B., "Performance of NEXT Engineering Model Power Processing Unit," AIAA Paper 2007-5214, July 2007.

[26] Patterson, M. J., and Oleson, S. R., "Low Power Propulsion for Small Spacecraft," AIAA Paper 1997-3060, July 1997.

[27] Hruby, V., Monheiser, J., Pote, B., Freeman, C., and Connolly, W., "Low Power, Hall Thruster Propulsion System," 26th International Electric Propulsion Conference, International Electric Propulsion Conference Paper 1999-092, 1999.

[28] Larson, W. J., and Wertz, J. R., *Space Mission Analysis and Design*, 3rd ed., Microcosm Press, New York, 1999, p. 711.

[29] Muller, J., "Thruster Options for Microspacecraft: A Review and Evaluation of Existing Hardware and Emerging Technologies," AIAA Paper 1997-3058, July 1997.

[30] Manzella, D., et al., "Evaluation of Low Power Hall Thruster Propulsion," AIAA Paper 1996-2736, July 1996.

[31] Humble, R. W., Henry, N. G., and Larson, W. J., *Space Propulsion Analysis and Design*, Revised, Primis Custom Publ., New York, 1995, pp. 179–294.

[32] Cengel, Y. A., and Boles, M. A., "Thermodynamics an Engineering Approach," 4th ed., McGraw–Hill, Boston, 2002, pp. 94–95.

[33] Ziemer, J. K., Randolph, T. M., Franklin, G. W., Hruby, V., Spence, D., Demmons, N., Roy, T., Ehrbar, E., Zwahlen, J., Martin, R., and Connolly, W., "Colloid Micro-Newton Thrusters for the Space Technology 7 Mission," *IEEE Aerospace Conference*, IEEE Paper 1234, Piscataway, NJ, March 2010.

[34] Paine, M., "Design Study for a Microfabricated Colloidal Thruster," M.S. Thesis, Aeronautics/Astronautics, Massachusetts Inst. of Technology Boston, 1999.

[35] Velasques, L., Akinwande, A. I., and Martínez-Sánchez, M., "A Microfabricated Colloidal Thruster Array," AIAA Paper 2002-3810, 2002.

[36] Tang, K., Lin, Y., Matson, D. W., Kim, T., and Smith, R., "Generation of Multiple Electrosprays Using Microfabricated Emitter Arrays for Improved Mass Spectrometric Sensitivity," *Analytical Chemistry*, Vol. 73, No. 8, 2001, pp. 1658–1663. doi:10.1021/ac001191r

A. Ketsdever
Associate Editor